*The Journal of Infectious Diseases*

MAJOR ARTICLE

# Peripheral Neuronopathy Associated With Ebola Virus Infection in Rhesus Macaques: A Possible Cause of Neurological Signs and Symptoms in Human Ebola Patients

**David X. Liu, Donna L. Perry, Timothy K. Cooper, Louis M. Huzella, Randy J. Hart, Amanda M. W. Hischak, John G. Bernbaum, Lisa E. Hensley, and Richard S. Bennett**

Integrated Research Facility, Division of Clinical Research, National Institute of Allergy and Infectious Diseases, National Institutes of Health, Frederick, Maryland, USA.

Neurological signs and symptoms are the most common complications of Ebola virus disease. However, the mechanisms underlying the neurologic manifestations in Ebola patients are not known. In this study, peripheral ganglia were collected from 12 rhesus macaques that succumbed to Ebola virus (EBOV) disease from 5 to 8 days post exposure. Ganglionitis, characterized by neuronal degeneration, necrosis, and mononuclear leukocyte infiltrates, was observed in the dorsal root, autonomic, and enteric ganglia. By immunohistochemistry, RNAscope in situ hybridization, transmission electron microscopy, and confocal microscopy, we confirmed that $CD68^+$ macrophages are the target cells for EBOV in affected ganglia. Further, we demonstrated that EBOV can induce satellite cell and neuronal apoptosis and microglial activation in infected ganglia. Our results demonstrate that EBOV can infect peripheral ganglia and results in ganglionopathy in rhesus macaques, which may contribute to the neurological signs and symptoms observed in acute and convalescent Ebola virus disease in human patients.

**Keywords.** Ebola virus; peripheral nervous system; sympathetic nervous system; parasympathetic nervous system; somatic ganglion; autonomic ganglion; dorsal root ganglion; enteric plexus.

Ebola virus (EBOV) is a nonsegmented negative-strand RNA virus in the family Filoviridae, classified as a risk group 4 pathogen, which causes severe hemorrhagic fever disease in humans and nonhuman primates (NHP) with fatality rates as high as 90% [1, 2]. The most common symptoms of Ebola virus disease (EVD) during the first week of illness are asthenia, diarrhea, nausea and vomiting, pain in the abdomen, lumbar and chest regions, arthralgia, and myalgia [3–7]. Some but not all clinical signs are reported in NHP models [8–10].

Patients with acute EVD can develop neurological symptoms as early as 7 days after the onset of clinical signs and central nervous system (CNS) involvement has been suggested [5, 11]. However, meningoencephalitis has only been diagnosed in survivors by computed tomography and magnetic resonance imaging [5, 12, 13]. Histopathologic evidence associated with EBOV in the CNS in EVD patients has not been reported [5]. Also, NHP studies of EVD do not report CNS involvement in animals succumbing to acute (<10 days) infection [8, 9, 14–16]. Profuse watery diarrhea with only mild inflammation in EVD patients suggests a primary secretory type diarrhea involving both the small and the large intestine rather than an inflammatory process [17, 18]. More than 41% of EVD patients show electrocardiographic (ECG) changes such as arrhythmias, which have been observed despite normal serum electrolytes and in the absence of pharmacologic agents [7, 19]. The profound neurologic signs and symptoms indicate peripheral nervous system involvement rather than CNS damage [5, 20].

The peripheral nervous system is composed of the somatic (or sensorimotor) and autonomic nervous system. Generally, the somatic nervous system, including dorsal root ganglia, is responsible for collecting sensory information and regulating effector organs that facilitate voluntary functions. The autonomic nervous system contains parasympathetic, enteric, and sympathetic components. The autonomic nervous system regulates the body's unconscious actions. The enteric nervous system governs the function of the gastrointestinal (GI) tract; while the sympathetic component stimulates the body's fight-flight-or-freeze response [21]. Sensory neuronopathy has been associated with many other viruses [22–25]. Damage to the parasympathetic ganglia has been reported in rhesus macaques that succumbed to Marburg virus infection and guinea pigs that succumbed to EBOV infection [26, 27].

Because postmortem CNS examination has not been reported in human EVD patients and shows no significant

Received 26 February 2020; editorial decision 23 May 2020; accepted 27 May 2020; published online June 4, 2020.

Correspondence: Lisa E. Hensley, PhD, MSPH, Integrated Research Facility, Division of Clinical Research, NIAID, NIH, B-8200 Research Plaza, Fort Detrick, Frederick, MD 21702 (lisa.hensley@nih.gov).

**The Journal of Infectious Diseases® 2020;222:1745–55**



DOI: 10.1093/infdis/jiaa304

histopathology in acute EBOV NHP models, this study aimed to examine the peripheral nervous system to aid in understanding of the pathogenesis underlying development of profound neurological signs and symptoms in EVD patients.

## METHODS

### Virus and Animals

Ebola virus/H.sapiens-tc/COD/1995/Kikwit-9 510 621 (GenBank: MG572235.1) was obtained from the Biodefense and Emerging Infections Research Resource Repository (BEI), National Institute of Allergy and Infectious Diseases (NIAID), National Institutes of Health (NIH) (catalog number NR-50 306). The virus was originally isolated from the blood sample from a fatal human patient in 1995 and passaged 3 times (Centers for Disease Control and Prevention number 807 223, University of Texas Medical Branch number WRC000121, and BEI number NR-596). The virus stock was diluted to a target dose of 1000 plaque forming units (PFU)/mL prior to inoculation without additional passaging at the Integrated Research Facility (IRF), NIAID.

Twelve (6 males and 6 females) 5- to 6-year-old rhesus macaques (*Macaca mulatta*) were inoculated intramuscularly (IM) with a target dose of 1000 PFU EBOV-Kikwit/animal into the left lateral triceps muscle. Two (1 male and 1 female) age-matched rhesus macaques served as uninfected controls and were inoculated IM with 1 mL of phosphate-buffered saline/animal at the same anatomic site. All macaques were observed for the development of clinical signs of EBOV infection and humanely euthanized when predetermined experimental endpoints were reached. All macaques used in this research project were cared for and used humanely according to the following policies: the US Public Health Service Policy on Humane Care and Use of Animals (2000); the Guide for the Care and Use of Laboratory Animals (1996); and the US Government Principles for Utilization and Care of Vertebrate Animals Used in Testing, Research, and Training (1985). All NIAID-IRF animal facilities and programs are accredited by the Association for Assessment and Accreditation of Laboratory Animal Care International. This study was performed in the Biosafety Level 4 Laboratory at the NIH/NIAID, Division of Clinical Research/IRF at Fort Detrick, Maryland.

### Histopathological Evaluation

Complete gross necropsy was performed and major organs (including cervical dorsal root ganglia [DRG]) were collected for histopathological examination and other assays. The autonomic ganglia associated with major organs (incidental collection) and enteric plexuses in the GI system were also examined in this study (Supplementary Tables 1–3). Tissues were fixed in 10% neutral-buffered formalin for at least 72 hours in biosafety level 4 containment prior to being routinely processed in a Tissue-Tek VIP-6 automated vacuum infiltration tissue processor (Sakura Finetek) followed by paraffin embedding with a Tissue-Tek model TEC unit (Sakura Finetek). Using a standard semiautomated rotary microtome and lighted water flotation bath (Leica Biosystems), paraffin-embedded tissues were sectioned at 4 μm, mounted on positively charged uncoated glass slides (ThermoFisher), air-dried at room temperature, and routinely stained with hematoxylin and eosin and coverslipped for histopathology, or stained via immunohistochemistry (IHC), RNAscope in situ hybridization (ISH), or confocal microscopy.

### Immunohistochemistry

IHC was performed on 4 μm thick, formalin-fixed, paraffin-embedded (FFPE) tissue sections using antibodies against EBOV matrix protein (VP40) and surface glycoprotein (GP), CD68, IBA1, cleaved caspase 3, and glial fibrillary acidic protein (GFAP). Primary and secondary antibodies and their sources, host, and type of antigen and working dilutions are listed in Supplementary Table 4. After primary antibody incubation, the tissues were treated with polymer-based secondary antibodies conjugated with alkaline phosphatase. Positive staining was visualized with Impact Vector Red chromogen (Vector Laboratories) and counterstained with hematoxylin.

### RNAScope In Situ Hybridization

To detect EBOV genomic RNA in 4-μm sections of FFPE tissues, in situ hybridization was performed using the manual RNAscope 2.5 HD RED kit (Advanced Cell Diagnostics) according to the manufacturer's instructions. Briefly, 20 ZZ probe pairs targeting the genomic EBOV-VP40 gene were designed and synthesized (Advanced Cell Diagnostics) for use as previously described [26]. As with IHC, the same semiquantitative 4-grade scale (Supplementary Table 1) was applied for ISH.

### Transmission Electron Microscopy

FFPE ganglia were processed for transmission electron microscopy (TEM) examination as previously described [28]. Briefly, sections 70 to 80 nm thick were collected on 200-mesh copper grids and post stained with Reynold's lead citrate. Samples were examined using a FEI Tecnai Spirit Twin transmission electron microscope (Thermo Fisher Scientific) operating at 80 kV.

### Confocal Microscopy

Selected ganglia were processed for confocal microscopy of EBOV-VP35 with CD68, IBA1, or GFAP as previously described [8]. Briefly, FFPE tissues were sectioned to 4 μm, mounted on charged glass slides, deparaffinized, then incubated with first unconjugated primary antibodies and followed by first fluorophore-conjugated secondary antibodies. The sections were then double-stained with secondary unconjugated primary antibodies and followed by secondary fluorophore-conjugated secondary antibodies. Primary and secondary antibodies and their sources, host, and type of antigen are listed in Supplementary Table 4. All fluorescent

images were obtained using a Leica SP5 TCS-2 confocal microscope with 405, 488, and 594-spectrum lasers activated (Leica Microsystems).

## RESULTS

### All Macaques Developed the Typical Clinical Signs and Succumbed to EBOV Disease

All 12 macaques that received a target dose of 1000 PFU of EBOV-Kikwit IM succumbed to EBOV disease. Eleven were euthanized and 1 was found dead shortly before the necropsy between 5 and 8 days post exposure (dpe). Preestablished euthanasia criteria allowed morbidity to serve as a surrogate for lethality. Typical clinical signs including fever, weakness, and decreased appetite developed as early as dpe 3 and increased in severity with time post exposure. Two (16.7%) macaques developed watery diarrhea at dpe 6 and 7, but the other 10 macaques showed constipation that varied in severity but was characterized by reduced to no stool at the late stages of disease. All macaques developed maculopapular skin rash that progressed from the face, arms, and thorax to a diffuse distribution terminally.

### EBOV Caused Sensory Neuron Degeneration and Necrosis

Cervical DRG were collected and examined from 8 of 12 rhesus macaques that succumbed with EVD as well as from 2 uninfected controls. All examined DRGs from macaques exposed to EBOV-Kikwit showed mild to severe neuronal degeneration and necrosis (Supplementary Table 1). Multifocally, some neurons were swollen with cytoplasmic vacuolization and loss of Nissl substance (chromatolysis, degeneration). Others were shrunken with pale-eosinophilic cytoplasm and angular nuclei (necrosis) (Figure 1B). Multifocally, the interstitium was mildly to moderately expanded by edema and infiltration of mononuclear leukocytes (Figure 1C). The stromal cells between the neurons in all the examined DRGs were weakly to strongly positive for EBOV-VP40 (Figure 1C) and EBOV-GP antigen by IHC and for viral genomic RNA by ISH (Figure 1D). The DRGs from the 2 uninfected controls (dpe 0) were morphologically within normal limits (Figure 1A) and negative for EBOV-VP40 and EBOV-GP by IHC and EBOV genomic RNA by ISH.

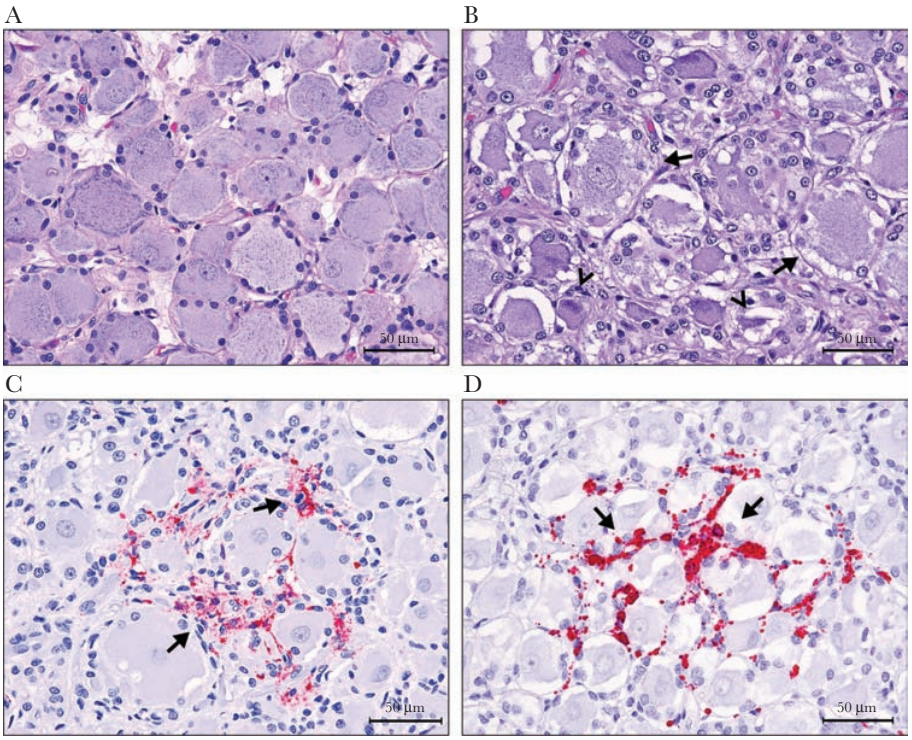


**Figure 1.** Histopathology, immunohistochemistry, and RNAScope-in situ hybridization of dorsal root ganglia (DRG). *A*, DRG from an uninfected macaque (nonhuman primate control [NHPc] 1, days post exposure [dpe] 0) shows normal, large-diameter neurons surrounded by a thin layer of small, round nuclei of supportive satellite cells. Hematoxylin and eosin stain. *B*, DRG from NHP 12 (dpe 8) that succumbed to Ebola-Kikwit infection shows marked neuronal degeneration and necrosis characterized by cytoplasmatic swelling and vacuolization and loss of Nissl substance (arrows) or shrunken cells with angular nuclei (^). Hematoxylin and eosin stain. *C*, Immunohistochemistry reveals that many stromal cells in the DRG (NHP 12, dpe 8) are strongly positive for Ebola-VP40 (arrows). *D*, RNAScope-in situ hybridization demonstrates that similar stromal cells in the DRG (NHP 12, dpe 8) are strongly positive (arrows) for Ebola genomic RNA.

#### EBOV Caused Autonomic Neuron Degeneration and Necrosis

Peripheral autonomic (parasympathetic) ganglia associated with major organs were incidentally collected and examined from the adrenal glands (8), hearts (7), seminal vesicles (5; Figure 2A), aortas (4), kidneys (4), urinary bladders (3), prostates (2), tracheas (2), uterine cervices (2), pancreata (2), and vagina (1) (Supplementary Table 2). Multifocally, mild to moderate neuronal degeneration and necrosis with infiltration of macrophages was present in most examined ganglia. Mild hemorrhage was noted in 3 (NHP 5, 11, and 12) of 5 ganglia from the seminal vesicle (Figure 2A) and in 1 (NHP 5) of 2 ganglia from the prostate gland. Rare intracytoplasmic inclusion bodies were noted in the stromal cells from the paradrenal ganglion (NHP 5).

Due to their small size, autonomic ganglia were not present in all serial sections from FFPE tissues and, as a result, were sometimes unavailable for downstream analysis. IHC and ISH demonstrated that stromal cells in most of the autonomic ganglia were multifocally weakly to strongly positive for EBOV-VP40 antigen (Figure 2B and 2C) and EBOV genomic RNA (Figure 2D), respectively. The ganglia (2 kidneys, 1 seminal vesicle, and 1 cervix) from the 2 uninfected controls were both EBOV-40 antigen and genomic RNA negative by IHC and ISH, respectively (Supplementary Table 2).

#### EBOV Caused Neuron Degeneration in Enteric Plexuses

Macroscopically and microscopically, acute, focal extensive hemorrhage was noted in the stomach (5 of 12) and duodenum (2 of 12). Multifocal, submucosal microthrombosis in the duodena was present in 11 of 12 macaques. One of 2 macaques (NHP 9) having watery diarrhea showed mild acute typhlitis. Otherwise, there was no significant inflammation observed in the GI tract in all other monkeys, including the other macaque (NHP 7) that exhibited watery diarrhea clinically.

However, multifocal, minimal to mild neuronal degeneration in enteric plexuses (both myenteric [Auerbach] and submucosal [Meissner]) was noted in stomachs (6 of 12), duodena (10 of 12), jejuna (7 of 12), ilia (6 of 12), ileocecal junctions (8 of 12; Figure 3A), ceca (6 of 12), and colons (6 of 12) (Supplementary Table 3). Multifocally, EBOV-VP40 antigen was detected by IHC in the stromal cells of enteric plexuses in the duodena (10 of 12) and other parts of the GI system (4 of 12 each, including 2 macaques exhibiting watery diarrhea) (Figure 3B). To confirm EBOV infection in the enteric plexuses, RNAscope-ISH was performed on all the sections (stomach to colon)

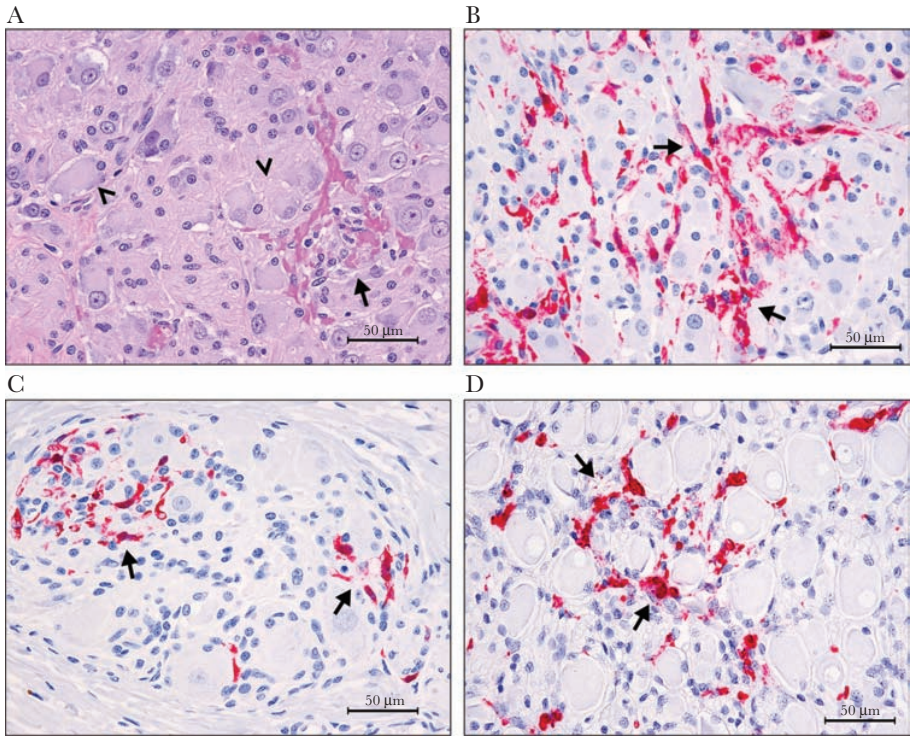


**Figure 2.** Histopathology, immunohistochemistry, and RNAScope-in situ hybridization of autonomic (parasympathetic) ganglia (AG). *A*, AG near the seminal vesicle from nonhuman primate (NHP) 5 (days post exposure [dpe] 7) that succumbed to Ebola-Kikwit infection shows multifocal, mild to moderate neuronal degeneration and necrosis (<) with hemorrhage and mononuclear cell infiltration (arrow). Hematoxylin and eosin stain. *B* and *C*, Immunohistochemistry shows that many stromal cells in the AG near the seminal vesicle (*B*) from NHP 11 (dpe 8) and the heart (*C*) from NHP 11 (dpe 8) are strongly positive for Ebola-VP40 (arrows). *D*, RNAScope-in situ hybridization demonstrates that many stromal cells in the AG near the adrenal gland from NHP 1 (dpe 5) are strongly positive for Ebola genomic RNA (arrows).

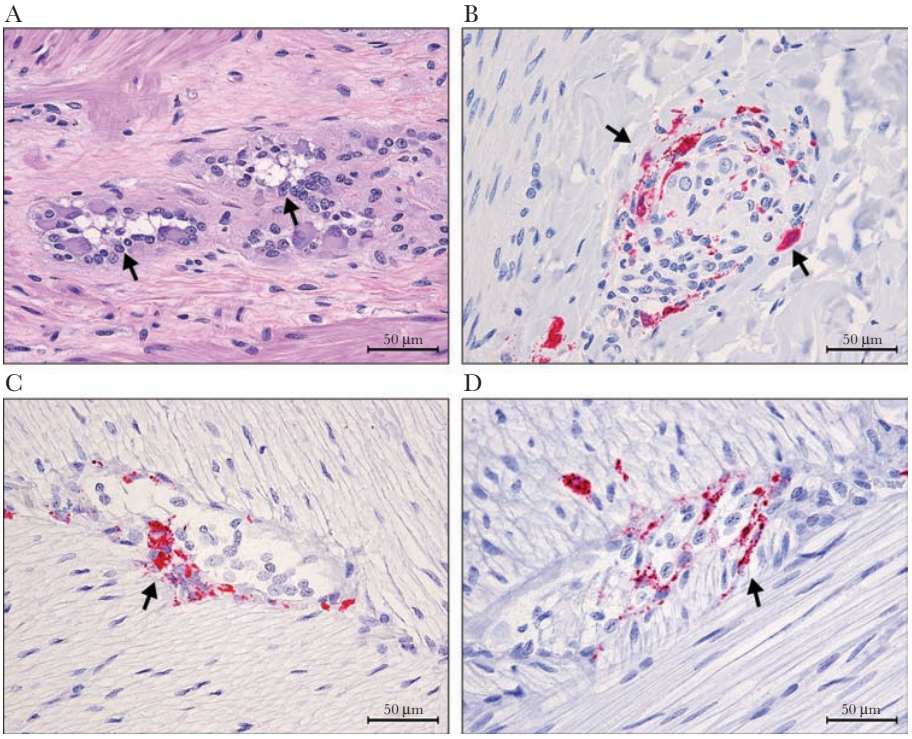


**Figure 3.** Histopathology, immunohistochemistry, and RNAScope-in situ hybridization from enteric plexuses in the gastrointestinal system. *A*, Meissner's plexus in the submucosa of ileoceco-junction from nonhuman primate (NHP) 8 (days post exposure [dpe] 7) that succumbed to Ebola-Kikwit infection shows mild to moderate, vacuolar neuronal degeneration (arrows). Hematoxylin and eosin stain. *B*, Immunohistochemistry shows that many stromal cells in a Meissner's plexus at ileoceco-junction (NHP 12, dpe 8) are strongly positive for Ebola-VP40 antigen (arrows). *C* and *D*, RNAscope-ISH reveals that many stromal cells in an enteric plexus in the duodenum of (*C*) NHP 11 (succumbed on dpe 8 without diarrhea) and (*D*) NHP 9 (succumbed on dpe 8 with diarrhea) are strongly positive for Ebola genomic RNA (arrow).

from 2 diarrheic macaques and the duodena from 2 nondiarrheic macaques. Multifocally, EBOV-RNA was detected in the stromal cells surrounding neurons in the enteric plexuses of all 4 macaques (2 diarrhea and 2 nondiarrhea) (Figure 3C and 3D and Supplementary Table 3).

#### CD68$^+$ macrophages Are the Target Cells for EBOV in Affected Dorsal Root and Autonomic Ganglia

Two DRGs from NHP 10 and 12 (dpe 8) and 2 autonomic ganglia from NHP 7 at dpe 7 (near an adrenal gland) and NHP 11 at dpe 8 (near a seminal vesicle) from FFPE tissues were examined by TEM. Mature, filamentous EBOV particles and intracytoplasmic EBOV inclusion bodies (nucleocapsid proteins forming typical EBOV filamentous nucleocapsid structures) were present in the macrophages adjacent to the neuronal perikaryon in all the seminal vesicle and adrenal ganglia examined (Figure 4A and 4B).

To confirm the cell type infected with EBOV in the DRG, tissue sections were double-immunostained for EBOV-VP35 and either CD68, IBA1, or GFAP, and examined using confocal microscopy. Colocalization of EBOV-VP35 with CD68 demonstrated that macrophages were the cell type harboring EBOV in peripheral ganglia (Figure 4C). However, there was no colocalization of EBOV (EBOV-VP35) in microglial cells (IBA1$^+$) or satellite cells (GFAP$^+$) observed in the examined ganglia.

#### Ebola Virus Infection Activates Microglial Cells in the Dorsal Root and Autonomic Ganglia

IHC for CD68 demonstrated that the number and intensity of CD68$^+$ macrophages increased mildly to markedly in the interstitium of all examined EBOV-infected ganglia (DRGs and autonomic ganglia) compared with controls (Figure 5A and 5B). Morphologically, the CD68$^+$ cells surrounding DRG neurons were large, plump/amoeboid with foamy cytoplasmic staining. It is noteworthy that the intensity of CD68$^+$ staining was weaker in the 2 terminal macaques euthanized at dpe 6 than in the 4 macaques euthanized at dpe 8. Generally, the number and intensity of CD68$^+$ staining positively correlated with neuronal damage. There were no CD68$^+$ macrophages in the ganglia from the uninfected controls.

On the contrary, the number and intensity of IBA1$^+$ cells were markedly reduced to absent in 4 macaques at dpe 8, although 2 macaques at dpe 6 showed either unchanged or slightly increased IBA1 staining when compared with uninfected controls. (Figure 5C and 5D) Morphologically, IBA1$^+$ cells were elongated with segmental staining (the ramified protrusions

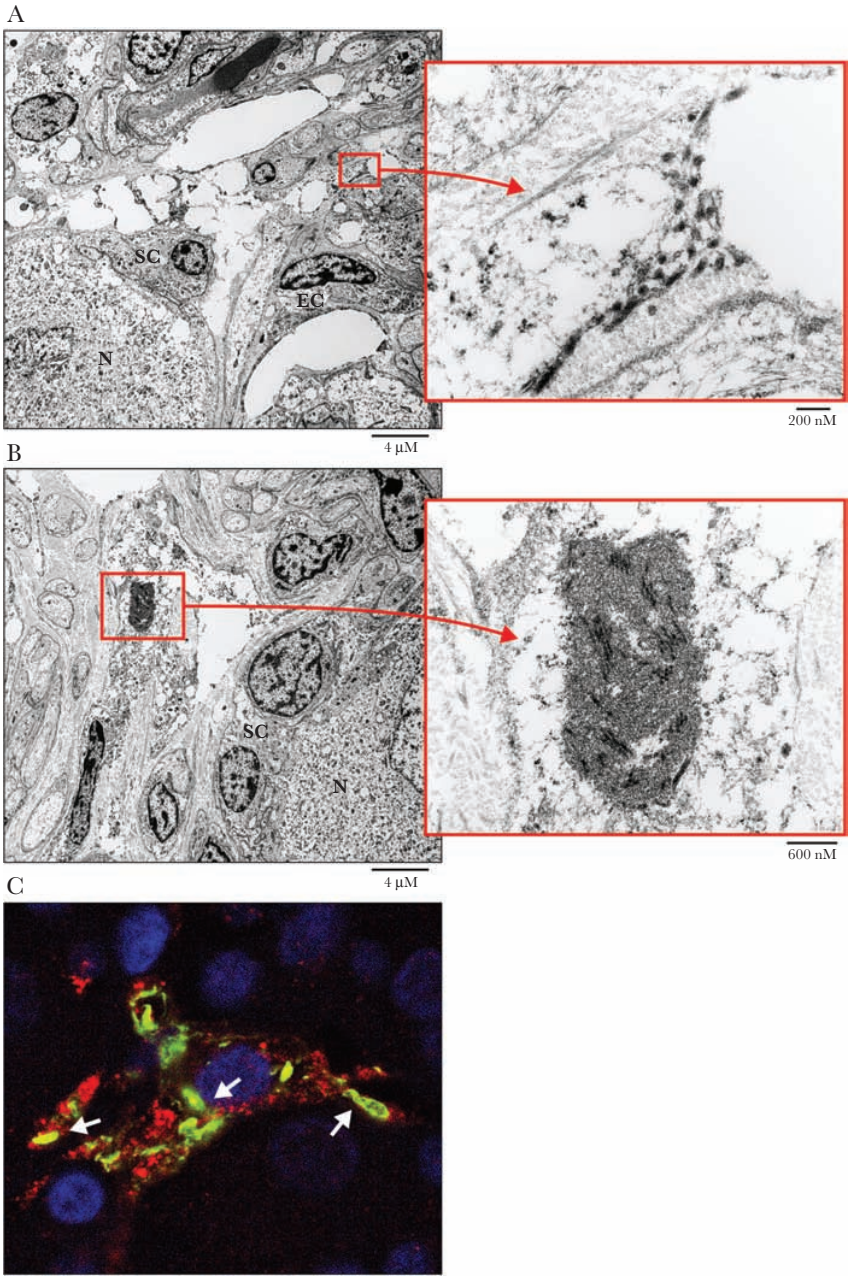


**Figure 4.** Transmission electron microscopy (TEM) and confocal microscopy of the ganglia from rhesus macaques that succumbed to Ebola-Kikwit infection. *A* and *B*, TEM shows mature, intercellular, filamentous EBOV particles (*A* and inset) and intracytoplasmic EBOV inclusion bodies (nucleocapsid proteins forming typical EBOV filamentous nucleocapsid structures) (*B* and inset) were present in a stromal cell adjacent to a neuronal perikaryon (N), satellite cells (SC), and endothelial cell (EC) in a ganglion near the seminal vesicle (nonhuman primate [NHP] 11, days post exposure 8). *C*, Confocal microscopy demonstrates the colocalization of EBOV-VP35 (Alexa Fluor 488, green) with CD68 (Alexa Fluor 594, red) in the macrophages (arrow) in the dorsal root ganglion from NHP 11.

from resting microglia) in the ganglia from uninfected controls (Supplementary Tables 1 and 2).

#### Ebola Virus Infection Induces Apoptosis and Satellite Cell Loss in the Sensory and Autonomic Ganglia

IHC demonstrated that cleaved caspase 3 staining increased mildly (neurons) to markedly (satellite cells) in the EBOV-infected peripheral ganglia when compared with the ganglia from uninfected controls (Figure 6A and 6B). Morphologically, the cleaved caspase 3 staining was intracytoplasmic with a clustered pattern of coarse granules. Generally, the positivity and intensity of cleaved caspase 3 staining correlated positively with ganglia neuronal degeneration and necrosis (Supplementary Tables 1 and 2). The weak,

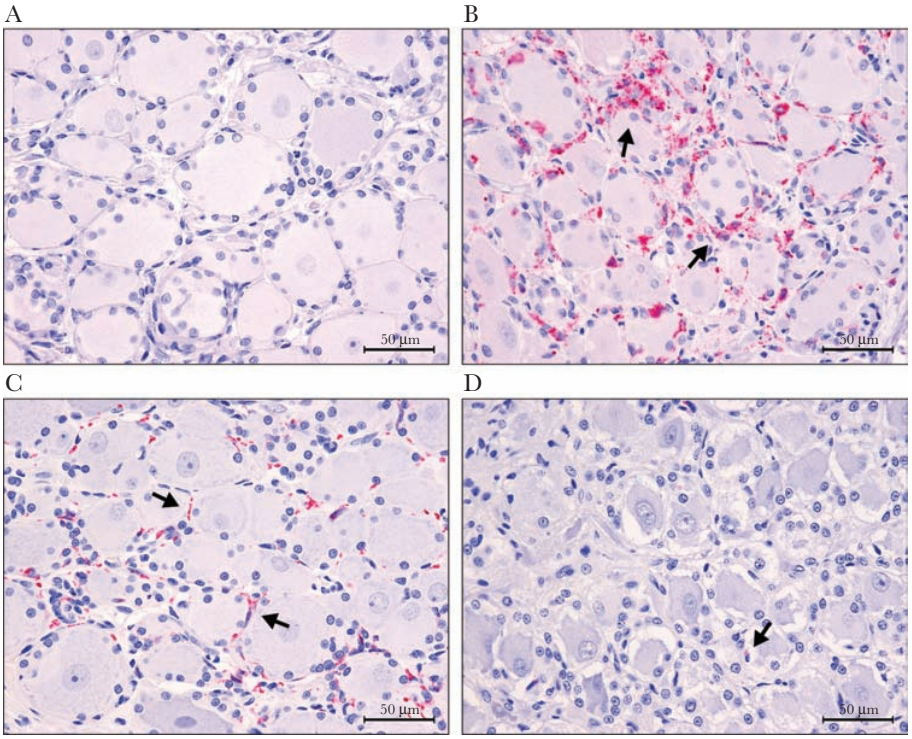


**Figure 5.** Immunohistochemistry for CD68 (*A* and *B*) and IBA1 (*C* and *D*) of dorsal root ganglion (DRG). *A*, DRG from nonhuman primate (NHPc 1 control at days post exposure [dpe] 0) is CD68 negative. *B*, Many interstitial plump/amoeboid cells surrounding degenerate neurons are CD68 positive (arrows) from a macaque (NHP 12) that succumbed to Ebola-Kikwit disease at dpe 8. *C*, DRG from an uninfected control (NHPc 1 at dpe 0) shows a normal, ramified, IBA1 positive staining cells (arrows) surrounding neurons. *D*, Macaque (NHP 12 at dpe 8) that succumbed to Ebola-Kikwit disease demonstrates a marked decrease to loss of IBA1 staining (arrow).

cloudy staining smeared in some neurons was interpreted as background staining, which is not uncommon in neuronal immunostaining [29].

On the contrary, the immunoprofile of GFAP in EBOV-infected peripheral ganglia decreased mildly to markedly, especially at the areas of neuronal degeneration and necrosis, when compared with that in the ganglia from uninfected controls (Figure 6C and 6D). The profile of GFAP staining in less affected areas was unchanged or slightly increased (Supplementary Tables 1 and 2).

## DISCUSSION

To date, there has been no documentation of peripheral neuropathy associated with acute EBOV infection in human patients or rhesus macaque models, although neurological dysfunction is one of the most common clinical signs and symptoms observed in acute human EVD. This study is the first to present evidence of systemic peripheral neuronopathy in rhesus macaques that succumbed to acute EBOV infection. Our results suggest that the neurological manifestations in human EVD patients are likely associated with peripheral ganglia neuronal damage due to EBOV infection.

To understand the pathogenesis of EVD is a challenge because it is one of the deadliest of epidemic viral diseases since its emergence in 1976 and studies are restricted to biosafety level 4 laboratories [20]. Although NHPs have been used as models of EVD for more than 40 years, there are still many unanswered questions underlying the pathogenesis of EVD [20, 30]. Neurological signs and symptoms of hypo- or hyperactive delirium, dysesthesia, hypothalamic dysfunction, seizures, and coma have been described in acute EVD, and CNS involvement is suggested [3, 5–7, 31]. However, meningoencephalitis associated with EBOV infection has only been diagnosed by magnetic resonance imaging, computed tomography, and/or cerebrospinal fluid polymerase chain reaction (PCR) month(s) later in survivors [5, 12, 13]. Nonhuman primate models of EVD have demonstrated no CNS involvement in macaques that succumbed to acute EBOV infection [8, 9, 14–16, 32]. Although edema and widespread glial nodules in the brains of 3 human patients that died of Marburg virus has been reported previously [33], the histopathological evidence of CNS damage in EVD patients are not available [5, 20].

Consistent with previous reports from the NHP model, EBOV infection of the CNS was not present in the current study [8, 9, 14–16]. The brains and spinal cords from all the

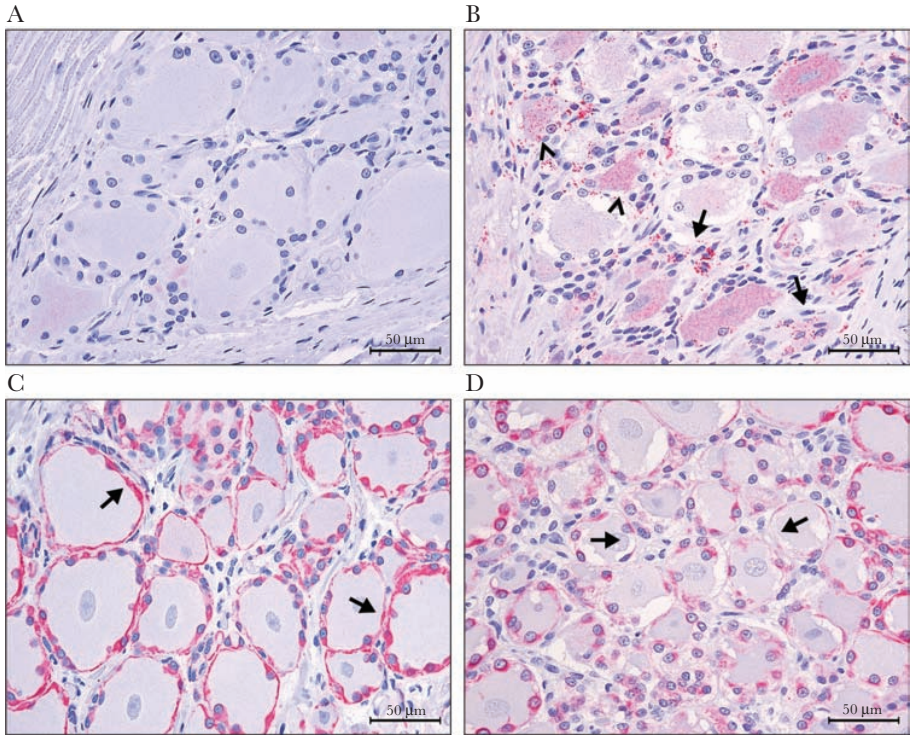


**Figure 6.** Immunohistochemistry of cleaved caspase 3 (*A* and *B*) and glial fibrillary acidic protein (GFAP) (*C* and *D*) in dorsal root ganglion (DRG). *A*, DRG from an uninfected control (nonhuman primate control [NHPc] 1 at days post exposure [dpe] 0) is cleaved caspase 3 negative (weak, minimal smeared staining is nonspecific background). *B*, Macaque (NHP 11) succumbed to Ebola-Kikwit disease at dpe 8 and demonstrates a marked increase in cleaved caspase 3 staining (granular apoptotic bodies) in the stomal cells (arrows, satellite cells) and neurons (<). *C*, Uninfected control (NHPc 1 at dpe 0) shows a strong GFAP staining (arrows) in the satellite cells surrounding neurons in the DRG. *D*, Macaque (NHP 11) that succumbed to Ebola-Kikwit disease at dpe 8 demonstrates a moderate decrease in GFAP staining (arrows) surrounding the degenerate neurons.

macaques were grossly and histopathologically unremarkable. There were no EBOV antigens (VP40 and GP) detected in the parenchyma of the brains. The spinal cords were also EBOV antigens and genomic RNA negative using IHC and ISH, respectively (data not shown). Instead, EBOV-infected macaques presented a significant sensory neuronopathy histopathologically. The profound neurological signs and symptoms, like ataxia, of EVD patients may be associated with peripheral sensory neuronopathy caused by EBOV infection. These conditions are probably exacerbated by electrolyte abnormalities, hypoglycemia, uremia, or hepatic hyperammonemia [20]. Degeneration of large sensory neurons, such as the DRG, can cause gait ataxia, proprioceptive sensory loss, and widespread deep tendon areflexia, whereas degeneration of small neurons and medium neurons presents as positive sensory symptoms, such as pain, "burning," allodynia, and hyperesthesia [34]. Similar clinical presentations associated with sensory neuronopathy caused by viral infections have also been reported [23, 24].

Damage to the autonomic and enteric plexuses ganglia has been associated with organ dysfunction, diarrhea, cardiac arrhythmias, and renal disease [35–37]. Approximately 50% of EBOV patients present with diarrhea [6], which is not an uncommon clinical sign in EBOV-infected NHPs [9, 38]. In the current study, 16.67% of macaques developed severe watery diarrhea. Acute typhlitis was only noted in 1 diarrheic macaque while the other showed no significant findings in its GI tract. However, EBOV antigen and/or genomic RNA were detected in the enteric plexuses of all macaques. Consistent with EVD patients, only slight inflammation in the lamina propria of the intestines in profound diarrheic macaques suggests a primary secretory rather than inflammatory process in the GI tract [16, 17, 39]. Myenteric nerve plexus dysfunction associated with viral infection has been documented [40].

About 41% of EVD patients transported to Europe or the United States showed ECG changes and there are many fatal arrhythmias in EVD patients in Western Africa [7, 19]. Electrolyte imbalance is an underlying concern. However, ECG change was documented in an EVD patient who had normal serum electrolytes and in the absence of any pharmacologic agents known to cause ECG changes [19]. Myocarditis or a predisposition for fatal arrhythmias has been speculated to be the cause of underlying abnormal ECG in EVD patients. However, there were no significant lesions in the

cardiovascular system in the current study, previous NHP models, or EVD human patients [8, 16, 20]. Interestingly, our study demonstrated that EBOV can cause autonomic ganglion cell damage in the cardiovascular system, which could contribute to the arrhythmias in EVD patients. Cardiovascular autonomic dysfunction has been associated with other viruses, like HIV and hepatitis C virus [41]. In this study, autonomic ganglionopathy associated with EBOV was also noted in the adrenal glands, prostate glands, seminal vesicles, kidneys, pancreata, tracheas, and cervix.

We also studied the mechanism of peripheral ganglionopathy in rhesus macaques with EVD. IHC demonstrated a marked increase in CD68 positivity, but a decrease in IBA1 expression (a protein expressed mainly in microglia) in EBOV-infected peripheral ganglia when compared to uninfected controls. The degree of change generally directly correlated with the severity of histopathologic changes and viral load. IBA1 provides a marker more suited for resident microglia in a normal physical condition, while CD68 reflects immune activation and response to tissue damage [42]. In addition, morphologically, microglial cells in uninfected controls and in less-affected ganglia were ramified with thin cytoplasmic processes and elongated nuclei, normal resting microglia [43], but they were plump in shape with round nuclei in EBOV-infected macaques. This morphological transformation and protein expression alterations suggest microglia activation, a pathological reaction in the affected ganglia [43–45]. However, the exact underlying mechanism of peripheral neuronopathy associated with EBOV infection is unclear. A similar phenomenon has been observed in Kupffer cells, resident macrophages in the liver, following EBOV infection [8, 20].

Furthermore, we also observed an increased cleaved caspase 3 staining in the affected ganglia, which suggested that EBOV can induce neuronal and satellite cell apoptosis. Additionally, there was markedly weaker GFAP (satellite cell marker) staining in the areas of more pronounced neuron degeneration and necrosis, especially in the macaques that succumbed to EBOV infection at dpe 8. Many previous studies have demonstrated that Ebola and Marburg viruses can induce apoptosis in multiple types of cells [46, 47]. Other viruses, such as herpes simplex virus type 2 and West Nile virus, can also induce glial cell apoptosis in the DRGs [48, 49]. A recent study demonstrated that a single inoculation of rVSVΔG-ZEBOV-GP virus in neonatal C57BL/6 mice resulted in a progressive apoptosis and neurodegeneration in the granular and Purkinje cells [50].

In summary, this study demonstrated that EBOV can cause systemic peripheral neuronopathy that likely contributes to the profound neurological signs seen in acute EVD patients.

## Supplementary Data

Supplementary materials are available at *The Journal of Infectious Diseases* online. Consisting of data provided by the authors to benefit the reader, the posted materials are not copyedited and are the sole responsibility of the authors, so questions or comments should be addressed to the corresponding author.

## Notes

***Acknowledgments.*** The authors thank James Logue, Becky Reeder, Russ Byrum, Dr Dan Ragland, Dr Marisa St. Claire, Maureen Abbott, and Nejra Isic for study organizing, animal care, and histology support; and Jiro Wada for figure preparation.

***Disclaimer***. The content of this article does not necessarily reflect the views or policies of the US Department of Health and Human Services or of the institutions and companies affiliated with the authors.

***Financial support.*** This work was supported in part through Battelle Memorial Institute's prime contract with the National Institute of Allergy and Infectious Diseases (NIAID) (contract number HHSN272200700016I); and by NIAID Interagency Agreement (grant number NOR15003-001-0000).

***Potential conflicts of interest.*** All authors: No reported conflicts of interest. All authors have submitted the ICMJE Form for Disclosure of Potential Conflicts of Interest. Conflicts that the editors consider relevant to the content of the manuscript have been disclosed.

## References

1. Kuhn JH, Bao Y, Bavari S, et al. Virus nomenclature below the species level: a standardized nomenclature for laboratory animal-adapted strains and variants of viruses assigned to the family Filoviridae. Arch Virol **2013**; 158:1425–32.
2. Sanchez A, Wagoner KE, Rollin PE. Sequence-based human leukocyte antigen-B typing of patients infected with Ebola virus in Uganda in 2000: identification of alleles associated with fatal and nonfatal disease outcomes. J Infect Dis **2007**; 196(suppl 2):S329–36.
3. Bwaka MA, Bonnet MJ, Calain P, et al. Ebola hemorrhagic fever in Kikwit, Democratic Republic of the Congo: clinical observations in 103 patients. J Infect Dis **1999**; 179(suppl 1):S1–7.
4. Aylward B, Barboza P, Bawo L, et al; WHO Ebola Response Team. Ebola virus disease in West Africa–the first 9 months of the epidemic and forward projections. N Engl J Med **2014**; 371:1481–95.
5. Chertow DS, Nath A, Suffredini AF, et al. Severe meningoencephalitis in a case of Ebola virus disease: a case report. Ann Intern Med **2016**; 165:301–4.
6. Schieffelin JS, Shaffer JG, Goba A, et al; KGH Lassa Fever Program; Viral Hemorrhagic Fever Consortium; WHO Clinical Response Team. Clinical illness and outcomes in patients with Ebola in Sierra Leone. N Engl J Med **2014**; 371:2092–100.
7. Chertow DS, Kleine C, Edwards JK, Scaini R, Giuliani R, Sprecher A. Ebola virus disease in West Africa–clinical manifestations and management. N Engl J Med **2014**; 371:2054–7.

8. Geisbert TW, Hensley LE, Larsen T, et al. Pathogenesis of Ebola hemorrhagic fever in cynomolgus macaques: evidence that dendritic cells are early and sustained targets of infection. Am J Pathol **2003**; 163:2347–70.
9. Baskerville A, Bowen ET, Platt GS, McArdell LB, Simpson DI. The pathology of experimental Ebola virus infection in monkeys. J Pathol **1978**; 125:131–8.
10. Larsen T, Stevens EL, Davis KJ, et al. Pathologic findings associated with delayed death in nonhuman primates experimentally infected with Zaire Ebola virus. J Infect Dis **2007**; 196(suppl 2):S323–8.
11. Sagui E, Janvier F, Baize S, et al. Severe Ebola virus infection with encephalopathy: evidence for direct virus involvement. Clin Infect Dis **2015**; 61:1627–8.
12. Howlett P, Brown C, Helderman T, et al. Ebola virus disease complicated by late-onset encephalitis and polyarthritis, Sierra Leone. Emerg Infect Dis **2016**; 22:150–2.
13. Jacobs M, Rodger A, Bell DJ, et al. Late Ebola virus relapse causing meningoencephalitis: a case report. Lancet **2016**; 388:498–503.
14. Jaax NK, Davis KJ, Geisbert TJ, et al. Lethal experimental infection of rhesus monkeys with Ebola-Zaire (Mayinga) virus by the oral and conjunctival route of exposure. Arch Pathol Lab Med **1996**; 120:140–55.
15. Jahrling PB, Geisbert JB, Swearengen JR, Larsen T, Geisbert TW. Ebola hemorrhagic fever: evaluation of passive immunotherapy in nonhuman primates. J Infect Dis **2007**; 196(suppl 2):S400–3.
16. Twenhafel NA, Mattix ME, Johnson JC, et al. Pathology of experimental aerosol Zaire Ebolavirus infection in rhesus macaques. Vet Pathol **2013**; 50:514–29.
17. Chertow DS, Uyeki TM, DuPont HL. Loperamide therapy for voluminous diarrhea in Ebola virus disease. J Infect Dis **2015**; 211:1036–7.
18. Emond RT, Evans B, Bowen ET, Lloyd G. A case of Ebola virus infection. Br Med J **1977**; 2:541–4.
19. Uyeki TM, Mehta AK, Davey RT Jr, et al; Working Group of the U.S.–European Clinical Network on Clinical Management of Ebola Virus Disease Patients in the U.S. and Europe. Clinical management of Ebola virus disease in the United States and Europe. N Engl J Med **2016**; 374:636–46.
20. Baseler L, Chertow DS, Johnson KM, Feldmann H, Morens DM. The pathogenesis of Ebola virus disease. Annu Rev Pathol **2017**; 12:387–418.
21. Catala M, Kubis N. Gross anatomy and development of the peripheral nervous system. Handb Clin Neurol **2013**; 115:29–41.
22. Volpi VG, Pagani I, Ghezzi S, Iannacone M, D'Antonio M, Vicenzi E. Zika virus replication in dorsal root ganglia explants from interferon receptor1 knockout mice causes myelin degeneration. Sci Rep **2018**; 8:10166.
23. Scaravilli F, Sinclair E, Arango JC, Manji H, Lucas S, Harrison MJ. The pathology of the posterior root ganglia in AIDS and its relationship to the pallor of the gracile tract. Acta Neuropathol **1992**; 84:163–70.
24. Burdo TH, Orzechowski K, Knight HL, Miller AD, Williams K. Dorsal root ganglia damage in SIV-infected rhesus macaques: an animal model of HIV-induced sensory neuropathy. Am J Pathol **2012**; 180:1362–9.
25. Lakritz JR, Bodair A, Shah N, et al. Monocyte traffic, dorsal root ganglion histopathology, and loss of intraepidermal nerve fiber density in SIV peripheral neuropathy. Am J Pathol **2015**; 185:1912–23.
26. Cooper TK, Sword J, Johnson JC, et al. New insights into Marburg virus disease pathogenesis in the rhesus macaque model. J Infect Dis **2018**; 218:423–33.
27. Cooper TK, Huzella L, Johnson JC, et al. Histology, immunohistochemistry, and in situ hybridization reveal overlooked Ebola virus target tissues in the Ebola virus disease guinea pig model. Sci Rep **2018**; 8:1250.
28. Liu DX, Perry DL, DeWald LE, et al. Persistence of Lassa virus associated with severe systemic arteritis in convalescing guinea pigs (*Cavia porcellus*). J Infect Dis **2019**; 219:1818–22.
29. Ellis J, Halliday G. A comparative study of avidin-biotin-peroxidase complexes for the immunohistochemical detection of antigens in neural tissue. Biotech Histochem **1992**; 67:367–71.
30. Feldmann H, Geisbert TW. Ebola haemorrhagic fever. Lancet **2011**; 377:849–62.
31. Kraft CS, Hewlett AL, Koepsell S, et al; Nebraska Biocontainment Unit and the Emory Serious Communicable Diseases Unit. The Use of TKM-100802 and convalescent plasma in 2 patients with Ebola virus disease in the United States. Clin Infect Dis **2015**; 61:496–502.
32. Wong G, Qiu X, Bi Y, et al. More challenges from Ebola: infection of the central nervous system. J Infect Dis **2016**; 214:294–6.
33. Kissling RE, Murphy FA, Henderson BE. Marburg virus. Ann N Y Acad Sci **1970**; 174:932–45.
34. Sghirlanzoni A, Pareyson D, Lauria G. Sensory neuron diseases. Lancet Neurol **2005**; 4:349–61.
35. Coumel P. Cardiac arrhythmias and the autonomic nervous system. J Cardiovasc Electrophysiol **1993**; 4:338–55.
36. Camilleri M. Disorders of gastrointestinal motility in neurologic diseases. Mayo Clin Proc **1990**; 65:825–46.
37. Sata Y, Head GA, Denton K, May CN, Schlaich MP. Role of the sympathetic nervous system and its modulation in renal hypertension. Front Med (Lausanne) **2018**; 5:82.
38. Bennett RS, Huzella LM, Jahrling PB, Bollinger L, Olinger GG Jr, Hensley LE. Nonhuman primate models of Ebola virus disease. Curr Top Microbiol Immunol **2017**; 411:171–93.

39. Martines RB, Ng DL, Greer PW, Rollin PE, Zaki SR. Tissue and cellular tropism, pathology and pathogenesis of Ebola and Marburg viruses. J Pathol **2015**; 235:153–74.
40. Istrate C, Hagbom M, Vikström E, Magnusson KE, Svensson L. Rotavirus infection increases intestinal motility but not permeability at the onset of diarrhea. J Virol **2014**; 88:3161–9.
41. Nzuobontane D, Ngu BK, Christopher K. Cardiovascular autonomic dysfunction in Africans infected with human immunodeficiency virus. J R Soc Med **2002**; 95:445–7.
42. Hendrickx DAE, van Eden CG, Schuurman KG, Hamann J, Huitinga I. Staining of HLA-DR, Iba1 and CD68 in human microglia reveals partially overlapping expression depending on cellular morphology and pathology. J Neuroimmunol **2017**; 309:12–22.
43. Waller R, Baxter L, Fillingham DJ, et al. Iba-1-/CD68$^{+}$ microglia are a prominent feature of age-associated deep subcortical white matter lesions. PLoS One **2019**; 14:e0210888.
44. Ito D, Imai Y, Ohsawa K, Nakajima K, Fukuuchi Y, Kohsaka S. Microglia-specific localisation of a novel calcium binding protein, Iba1. Brain Res Mol Brain Res **1998**; 57:1–9.
45. Graeber MB, López-Redondo F, Ikoma E, et al. The microglia/macrophage response in the neonatal rat facial nucleus following axotomy. Brain Res **1998**; 813:241–53.
46. Baize S, Leroy EM, Mavoungou E, Fisher-Hoch SP. Apoptosis in fatal Ebola infection. Does the virus toll the bell for immune system? Apoptosis **2000**; 5:5–7.
47. Geisbert TW, Hensley LE, Gibb TR, Steele KE, Jaax NK, Jahrling PB. Apoptosis induced in vitro and in vivo during infection by Ebola and Marburg viruses. Lab Invest **2000**; 80:171–86.
48. Ozaki N, Sugiura Y, Yamamoto M, Yokoya S, Wanaka A, Nishiyama Y. Apoptosis induced in the spinal cord and dorsal root ganglion by infection of herpes simplex virus type 2 in the mouse. Neurosci Lett **1997**; 228:99–102.
49. Samuel MA, Morrey JD, Diamond MS. Caspase 3-dependent cell death of neurons contributes to the pathogenesis of West Nile virus encephalitis. J Virol **2007**; 81:2614–23.
50. McWilliams IL, Kielczewski JL, Ireland DDC, et al. Pseudovirus rVSVDeltaG-ZEBOV-GP infects neurons in retina and CNS, causing apoptosis and neurodegeneration in neonatal mice. Cell Reports **2019**; 26:1718–26.e4.